BRAIN COMMUNICATIONS

Gain-of-function *GABRB3* variants identified in vigabatrin-hypersensitive epileptic encephalopathies

Nathan L. Absalom,[1] Vivian W. Y. Liao,[1] Kavitha Kothur,[2] Dinesh C. Indurthi,[1,*] Bruce Bennetts,[3,4] Christopher Troedson,[5] Shekeeb S. Mohammad,[2] Sachin Gupta,[5] Iain S. McGregor,[6] Michael T. Bowen,[6] Damien Lederer,[7] Sandrine Mary,[7] Liesbeth De Waele,[8] Katrien Jansen,[8] Deepak Gill,[2] Manju A. Kurian,[9,10] Amy McTague,[9,10] Rikke S. Møller,[11,12] Philip K. Ahring,[1] Russell C. Dale[2] and Mary Chebib[1]

*Present address: Department of Physiology and Biophysics, Jacobs School of Medicine and Biomedical Sciences, University at Buffalo, NY 14203, USA.

Variants in the *GABRB3* gene encoding the β3-subunit of the γ-aminobutyric acid type A (receptor are associated with various developmental and epileptic encephalopathies. Typically, these variants cause a loss-of-function molecular phenotype whereby γ-aminobutyric acid has reduced inhibitory effectiveness leading to seizures. Drugs that potentiate inhibitory GABAergic activity, such as nitrazepam, phenobarbital or vigabatrin, are expected to compensate for this and thereby reduce seizure frequency. However, vigabatrin, a drug that inhibits γ-aminobutyric acid transaminase to increase tonic γ-aminobutyric acid currents, has mixed success in treating seizures in patients with *GABRB3* variants: some patients experience seizure cessation, but there is hypersensitivity in some patients associated with hypotonia, sedation and respiratory suppression. A *GABRB3* variant that responds well to vigabatrin involves a truncation variant (p.Arg194*) resulting in a clear loss-of-function. We hypothesized that patients with a hypersensitive response to vigabatrin may exhibit a different γ-aminobutyric acid A receptor phenotype. To test this hypothesis, we evaluated the phenotype of *de novo* variants in *GABRB3* (p.Glu77Lys and p.Thr287Ile) associated with patients who are clinically hypersensitive to vigabatrin. We introduced the *GABRB3* p.Glu77Lys and p.Thr287Ile variants into a concatenated synaptic and extrasynaptic γ-aminobutyric acid A receptor construct, to resemble the γ-aminobutyric acid A receptor expression by a patient heterozygous for the *GABRB3* variant. The mRNA of these constructs was injected into *Xenopus* oocytes and activation properties of each receptor measured by two-electrode voltage clamp electrophysiology. Results showed an atypical gain-of-function molecular phenotype in the *GABRB3* p.Glu77Lys and p.Thr287Ile variants characterized by increased potency of γ-aminobutyric acid A without change to the estimated maximum open channel probability, deactivation kinetics or absolute currents. Modelling of the activation properties of the receptors indicated that either variant caused increased chloride flux in response to low concentrations of γ-aminobutyric acid that mediate tonic currents. We therefore propose that the hypersensitivity reaction to vigabatrin is a result of *GABRB3* variants that exacerbate GABAergic tonic currents and caution is required when prescribing vigabatrin. In contrast, drug strategies increasing tonic currents in loss-of-function variants are likely to be a safe and effective therapy. This study demonstrates that functional genomics can explain beneficial and adverse anti-epileptic drug effects, and propose that vigabatrin should be considered in patients with clear loss-of-function *GABRB3* variants.

1 Faculty of Medicine and Health, School of Pharmacy, Brain and Mind Centre, The University of Sydney, Sydney, New South Wales 2006, Australia
2 Kids Neuroscience Centre at The Children's Hospital at Westmead, Westmead, New South Wales 2145, Australia
3 Department of Molecular Genetics, The Children's Hospital at Westmead, Westmead, New South Wales 2145, Australia

Received March 19, 2020. Revised July 31, 2020. Accepted August 28, 2020. Advance Access publication October 1, 2020

4 Discipline of Paediatrics and Adolescent Health, The Children's Hospital at Westmead Clinical School, The University of Sydney, 2145, Australia
5 T.Y. Nelson Department of Neurology and Neurosurgery, The Children's Hospital at Westmead, Westmead, New South Wales 2145, Australia
6 Faculty of Science, Lambert Initiative for Cannabinoid Therapeutics, Brain and Mind Centre, The University of Sydney, Sydney, New South Wales 2006, Australia
7 Institute of Pathology and Genetics, Center for Human Genetics, Gosselies 6041, Belgium
8 Department of Development and Regeneration, KULeuven, Leuven 3000, Belgium
9 Molecular Neurosciences, UCL Great Ormond Street Institute of Child Health, London WC1E 6BT, UK
10 Department of Neurology, Great Ormond Street Hospital for Children, London WC1N 3JH, UK
11 Department of Epilepsy Genetics and Personalized Medicine, Danish Epilepsy Centre, Dianalund 4293, Denmark
12 Department of Regional Health Research, University of Southern Denmark, Odense 5230, Denmark

Correspondence to: Dr Nathan Absalom, PhD
E-mail: nathan.absalom@sydney.edu.au

Correspondence may also be addressed to: Prof Mary Chebib, PhD.
E-mail: mary.collins@sydney.edu.au

Keywords: developmental and epileptic encephalopathies; $GABA_A$ receptor; gain-of-function variants; vigabatrin; benzodiazepines

Abbreviations: DEEs = developmental and epileptic encephalopathies; Est Po = estimated receptor open probability;GABA = γ-aminobutyric acid; WT = wild-type.

Graphical Abstract

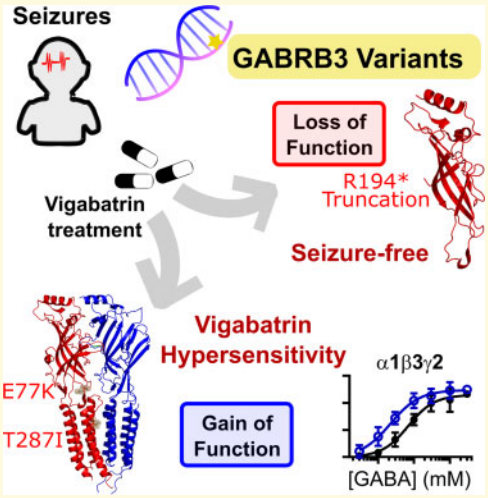

Introduction

Developmental and epileptic encephalopathies (DEEs) are a group of severe childhood epilepsies often associated with co-morbidities including developmental delay (DD), intellectual disability, movement disorders and autistic features (French, 2006). Variants in the *GABRB3* gene that code for $\beta3$ γ-aminobutyric acid type A ($GABA_A$) receptor subunits are associated with DEE (Johannesen *et al.*, 2016; Møller *et al.*, 2016; Absalom *et al.*, 2019; Hernandez *et al.*, 2019; Maljevic *et al.*, 2019).

$GABA_A$ receptors are ligand-gated ion channels that regulate neurotransmission via the inhibitory neurotransmitter, GABA. Nineteen genes code for subunits that make up the various $GABA_A$ receptor subtypes. These subunits mix and match to form distinct receptor subtypes (Johannesen *et al.*, 2016; Liao *et al.*, 2019) that express at different cellular and brain regions to regulate neurophysiological responses such as movement, learning and memory.

The $\beta3$ subunit of the $GABA_A$ receptor is widely expressed across many regions of the brain (Fritschy *et al.*, 1992; Persohn *et al.*, 1992; Wisden and Seeburg, 1992; Pirker *et al.*, 2000) often combining with various α subunits (such as $\alpha1$) and $\gamma2$ subunits to form pentameric synaptic $GABA_A$ receptors with a $2\alpha:2\beta:\gamma$ stoichiometry (Fig. 1A). These receptors respond to high levels of synaptically released GABA to mediate a phasic response. In addition, the $\beta3$ subunit is found at extrasynaptic sites, combining with either $\alpha5$ or δ subunits resulting in extrasynaptic receptors that respond to comparatively low levels of GABA to mediate a tonic GABAergic response.

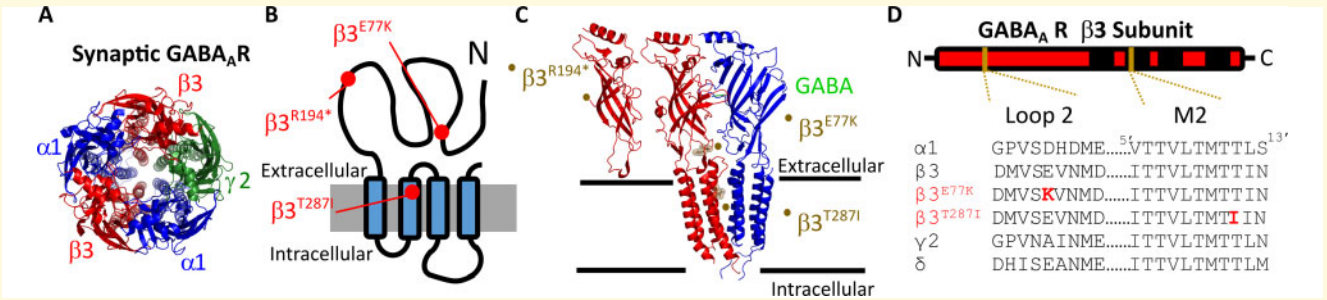

Figure 1 Structural location of GABA$_A$ receptor variants. (**A**) Pentameric structure from the extracellular side of the membrane of the α1β3γ2 synaptic GABA$_A$ receptor (Masiulis *et al.*, 2019). α1 subunits are in blue, β3 in red and γ2 in green. (**B**) Schematic of a single β3 GABA$_A$ receptor showing the location of the β3^{E77}, β3^{R194} and β3^{T287} residues (red) in the extracellular and the four transmembrane domains M1–M4 (black). (**C**) Also shown is the structure of the interface between β3 and α1 subunits from side-on showing the truncation of the β3^{R194}* subunit, the structure displaying the β3^{E77} residue (black sticks and spheres) in the coupling region connecting the extracellular domain and the transmembrane domains, and the β3^{T287} residue (black sticks and spheres) at the top of the pore lining M2 region. (**D**) The sequence alignment for selected subunits is shown below in the loop 2 and M2 regions that contain the β3^{E77K} and β3^{T287I} variants, respectively (red).

As GABA$_A$ receptors work to maintain normal brain function, genetic variants in individual genes such as the *GABRB3* can lead to neurophysiological dysfunction including seizure disorders such as febrile seizures, generalized epilepsy with febrile seizures+, myoclonic atonic epilepsy, West syndrome, Dravet syndrome and other severe unclassified DEEs (Johannesen *et al.*, 2016; Møller *et al.*, 2016; Absalom *et al.*, 2019; Hernandez *et al.*, 2019; Maljevic *et al.*, 2019). An analysis of the known variants in GABA$_A$ receptors proposed that most variants lead to loss-of-function molecular phenotypes through impaired transcription or translation, misfolding and degradation, endoplasmic reticulum retention of truncated or functional receptors or impairments in receptor activation (Hernandez and Macdonald, 2019). However, increased GABAergic activity can also lead to seizure phenotypes, such as in loss-of-function *SLC6A1* variants (Mattison *et al.*, 2018), and loss-of-function GABA$_A$ receptor molecular phenotypes cannot simply be assumed. Nevertheless, with the prevalence of loss-of-function GABA$_A$ receptor variants, drugs that enhance GABAergic neurotransmission could be expected to help reduce seizures in these patients, yet many patients with DEE are either refractory to current treatments or they worsen symptoms or cause a severe adverse reaction.

Vigabatrin is an irreversible GABA transaminase inhibitor used as adjunctive therapy for focal seizures and monotherapy for infantile spasms. It is thought to alleviate seizures by increasing tonic, or persistent, GABAergic inhibitory currents (Wu *et al.*, 2001, 2003). Therefore, it may be anticipated that vigabatrin would be useful in patients with *GABRB3* variants that have a reduction in the number or a functional impairment of *β3*-containing GABA$_A$ receptors.

However, recent reports described two patients presenting with *GABRB3* variants that responded adversely to vigabatrin. When administered vigabatrin, these patients responded with reduced seizures but suffered severe adverse effects, such as decreased alertness, extreme drowsiness, hypotonia, sedation and respiratory difficulties, that reversed upon treatment cessation. Next-generation sequencing identified the *GABRB3* variants p.Glu77Lys and p.Thr287Ile (Papandreou et al., 2016; Kothur *et al.*, 2018). Our hypothesis is that the adverse responses to vigabatrin are a consequence of the molecular phenotype of the individual *GABRB3* variants.

In this study, we sought to determine whether the molecular phenotype of the variants could explain the patients hypersensitivity to vigabatrin. Our results demonstrated that patients who responded adversely to vigabatrin had atypical gain-of-function molecular phenotypes when compared to patients that responded well to vigabatrin who had typical loss-of-function phenotype. We propose that functionally analysing variants of patients is essential to avoid adverse effects when prescribing drug treatments.

Materials and methods

This study was performed in accordance with ethical principles for medical research outlined in the Declaration of Helsinki. All genetic studies were performed with informed consent of the patients or their responsible relatives and were approved by the local ethical committees. All procedures using *Xenopus laevis* frogs and harvesting of oocytes were approved by the animal ethics committee of the University of Sydney (animal ethics committee No. 2016/970) in accordance with the National Health and Medical Research Council of Australia code for the care and use of animals. Frogs were housed in custom-built tanks with a plastic shelter, with three frogs to a tank. Water was reticulated and water quality checked weekly. Frogs were fed twice weekly with Wardley's reptile sticks

(Wardley, USA) and Irradiated Adult Xenopus Diet (Xenopus Express, Florida, USA).

Patients

We report the electrophysiological effects of variants previously reported and the detailed clinical case of two previously reported and one novel *GABRB3* gene variant (maternally inherited with the affected relative included) (Papandreou et al., 2016; Kothur *et al.*, 2018). We chose to analyse patients on the following criteria: one variant identified as loss-of-function (novel variant p. Arg194*) associated with a favourable response to vigabatrin; and two variants (p.Glu77Lys and p.Thr287Ile) associated with the adverse reaction of hypersensitivity to vigabatrin (Papandreou et al., 2016; Kothur *et al.*, 2018).

Electrophysiological analyses were performed for two *GABRB3* variants and compared to the wild-type (WT) to correlate their functional response to their pharmacoresponse to vigabatrin and nitrazepam where used.

Molecular biology

The human concatenated γ2-β3-α1-β3-α1 receptor construct has previously been described (Absalom *et al.*, 2019; Liao *et al.*, 2019). The γ2-β3-α5-β3-α5 subunit was created by subcloning α5 subunits with flanking linker sequences into the γ2-β3-α1-β3-α1 construct. Briefly, vectors containing DNA encoding the α5 subunits with linker sequences and unique restriction sites were purchased from Genscript (Singapore). The α5 subunits were cut and β3 subunits were ligated with the vector containing the γ2 subunit to create concatenated receptors with linker sequences in the order of γ2-$(AGS)_5$-β3-$(AGS)_5$LGS(AGS)-α5-AGT$(AGS)_5$-β3-$(AGS)_4$ATGAGS-α5.To create $\beta3^{E77K}$ and $\beta3^{T287I}$ sets of concatenated receptors, human cDNA for monomeric β3 $GABA_A$ receptor subunits were mutated using QuikChange II Site Directed Mutagenesis Kit (Agilent Technologies, Mulgrave, Australia) then subcloned into the γ2-β3-α1-β3-α1 or The γ2-β3-α5-β3-α5 construct using unique restriction sites. Fidelity of all coding sequences were verified by double stranded sequencing. DNA gel electrophoresis ensured incorporation of the five subunits. cRNA was produced from linearized cDNA using the mMessage mMachine T7 Transcription kit (Thermo Fisher, Scoresby, Australia).

Xenopus surgery and oocyte preparation

In brief, a section of ovarian lobe from *X. laevis* was surgically removed under anaesthesia induced by tricaine, cut and digested with 35 mg of collagenase-A in 15 ml OR2 (in mM: NaCl, 82.5; HEPES, 5; $MgCl_2$, 2 and KCl, 2; pH 7.4) at 18°C for ~1 h until oocytes were fully detached. Oocytes were then injected with 2 ng of cRNA per cell encoding a concatenated receptor and incubated for 2–4 days at 18°C in ND96 solution (in mM: NaCl, 96; KCl, 2; $MgCl_2$, 1; $CaCl_2$, 1.8; HEPES, 5; pH 7.4) supplemented with 2.5 mM pyruvate, 0.5 mM theophylline and 50 µg/ml gentamicin.

Two-electrode voltage-clamp recording

Cell currents were recorded using the two-electrode voltage-clamp method as previously described (Absalom *et al.*, 2019). Briefly, cells were impaled with microelectrodes filled with 3 M KCl then voltage clamped at −60 mV. Currents were recorded using a GeneClamp 500B (Axon Instrument, Foster City, USA) or OC-725C amplifier Clamp (Warner Instrument Corp., Hamden, USA) and digitized with a Powerlab 8/36 and LabChart version 8.03 (ADInstruments, Sydney, Australia).

For concentration–response curves and estimated open probability (Est P_{Omax}), a 3 mM concentration of GABA was applied as a reference three times and peak currents were normalized to the mean current of the last two GABA applications. When estimating P_{Omax}, after three consecutive applications of reference 3 mM GABA solution, 10 mM GABA, 1 µM diazepam and 3 µM etomidate was co-applied at γ2-β3-α1-β3-α1 and 10 mM GABA and 10 µM etomidate was co-applied at γ2-β3-α5-β3-α5 receptors. A washout period of 10–12 min was performed between GABA applications to prevent effects from desensitization. Experiments were performed over a minimum of two different batches of oocytes.

Receptor desensitization assay

To measure current decay rates, dead volume was reduced and single concentrations of GABA were applied for 120 s. Traces were fitted to an exponential decay in GraphPad Prism (v8).

Data analysis and statistics

Concentration–response curves were fitted using GraphPad Prism 8 to a monophasic Hill equation of the form:

$$I = I_{max}\left(\frac{[A]^{n_H}}{[A]^{n_H} + EC_{50}{}^{n_H}}\right),$$

where I_{max} is the maximum current, EC_{50} is the concentration eliciting half-maximum response, $[A]$ is the ligand concentration and n_H is the Hill slope. Individual oocytes where a complete concentration–response curve was taken are recorded as a single n. Responses were normalized to the fitted maximum response of individual curves. The EC_{50} is from the fitting of Hill equations to all data, while the $logEC_{50}$, I_{max} and n_H values are the mean and

error derived from fitting curves to individual experiments.

For nitrazepam concentration–response curves, the per cent modulation was derived by the equation:

$$\text{Per cent Modulation} = 100 \times \frac{I_{\text{Nitrazepam}} - I_{\text{GABA EC10}}}{I_{\text{GABA EC10}}}$$

and fitted to the Hill equation for parameters of the curves.

The Estimated P_{Omax} for individual experiments was derived by the equation:

$$\text{Est. } Po_{max} = \frac{I_{3\text{mM GABA}}}{I_{3\text{mM GABA 1}\mu\text{M Diazepam 3}\mu\text{M Etomidate}}}.$$

To determine the decay rates, individual traces from the peak current were fitted to the equation:

$$I = (I_0 - \text{Plateau})e^{-kt} + \text{Plateau},$$

where I is the current at time t, I_0 is the current at time point 0, Plateau is the current at steady-state desensitization and k is the decay constant.

The modelled response was determined by assuming an equal expression ratio (1:1:1:1) of WT, γ-$\beta3^{\bullet}$-α-$\beta3$-α, γ-$\beta3$-α-$\beta3^{\bullet}$-α and γ-$\beta3^{\bullet}$-α-$\beta3^{\bullet}$-α receptors and given by the equation:

$$\begin{aligned}\text{Modelled Response} = 0.25 \times (&\text{Est Po(wt)} \times \frac{[A]^{nH(wt)}}{[A]^{nH(wt)} + EC_{50wt}} + \text{Est Po(1)} \times \frac{I_{3\text{mM GABA(1)}}}{I_{3\text{mM GABA(wt)}}} \frac{[A]^{nH(1)}}{[A]^{nH(1)} + EC_{50(1)}} + \\ &\text{Est Po(2)} \times \frac{I_{3\text{mM GABA(2)}}}{I_{3\text{mM GABA(wt)}}} \frac{[A]^{nH(2)}}{[A]^{nH(2)} + EC_{50(2)}} \\ &+ \text{Est Po(3)} \times \frac{I_{3\text{mM GABA(3)}}}{I_{3\text{mM GABA(wt)}}} \frac{[A]^{nH(3)}}{[A]^{nH(3)} + EC_{50(3))}}\end{aligned}$$

,where the Est Po(wt), n_H(wt) and EC_{50}wt are the Est Po_{max}, Hill co-efficient and EC_{50} of the wild-type receptor, Est Po(1), $n_H(1)$ and $EC_{50(1)}$ are the respective parameters of the γ-$\beta3^{\bullet}$-α-$\beta3$-α receptor, Est Po(2), $n_H(2)$ and $EC_{50(2)}$ are respective parameters of the γ-$\beta3$-α-$\beta3^{\bullet}$-α receptor Est Po (3), $n_H(3)$ and $EC_{50(3)}$ are the respective of the γ-$\beta3^{\bullet}$-α-$\beta3^{\bullet}$-α receptors.

The change in response was determined by subtracting the WT concentration–response curve. The GABA concentration that vigabatrin induces was increased by 30-fold to compensate for the higher EC_{50} values determined using concatenated receptors expressed in oocytes compared to free subunits expressed in recombinant mammalian cells (Mortensen *et al.*, 2011).

For statistical analysis, Est P_{Omax} values and parameters derived from concentration–response curves were compared with a one-way ANOVA with Tukey's *post hoc* test. Significance values of $P < 0.05$, $P < 0.01$ and $P < 0.001$ are shown in the results section. For desensitization, the decay rates were plotted against $\log_{10}$ GABA concentrations and fitted to a linear curve. An *F*-test was performed to determine if the relationship between the decay constants and GABA concentration for each variant and the WT could be described by a single curve. If not, a Mann–Whitney test was then performed to determine if the data were significantly different between the WT and variant receptors. Power calculations were performed for comparisons between maximum currents, $\log EC_{50}$s and Est Po_{max} with a one-way ANOVA with an estimated effect size of 0.5, power of 0.85 and a significance level of 0.05 for a minimum number of experiments of 9.

Blinding and randomization

Experiments were not blinded or randomized, but performed on a semi-automated recording apparatus that enabled four experiments to be performed at any one time.

Data availability

Raw data are available on request.

Results

Patient that responds to vigabatrin without hypersensitivity

The vigabatrin-responsive patient chosen represented a typical loss-of-function *GABRB3* variants that was prescribed vigabatrin as monotherapy. This variant is a novel case of a maternally-inherited truncation variant p. Arg194* (cases 1 and 2). This variant leads to an aberrant protein sequence of the affected $\beta3$ subunit, and the resultant truncated protein cannot express the critical extracellular and pore-forming transmembrane motifs. Hence, these patients would only have functional $\beta3$ subunits from the unaffected allele.

Clinical details of patient and affected mother that responds to vigabatrin without hypersensitivity

Cases 1 and 2 (p.Arg194*) are a 29 month old girl and her affected mother. The girl presented with infantile spasms at the age of 7 months. EEG at onset showed hypsarrhythmia, which later evolved into multifocal discharges. Introduction of vigabatrin was tolerated without side effect but was not sufficient to achieve seizure control and prednisolone was added with good effect. In the following period she was seizure free on monotherapy with 130 mg/kg vigabatrin, which was later switched to valproic acid. At last reported follow-up at 21 months of

age she had global DD and a right-sided hemiplegia. She could sit unsupported in a kyphotic position and was able to say a few words. The mother of the patient presented with atonic and generalized tonic clonic seizures at the age of two years. She was treated with valproic acid with good effect and has been seizure free since the age of 18 years. She has never tried vigabatrin. She has mild learning difficulties.

Molecular phenotype of vigabatrin-responsive patients without hypersensitivity

The $\beta3^{R194*}$ truncation variant can be safely predicted to have a loss-of-function molecular phenotype. The $\beta3^{R194*}$ variant introduces a stop codon within the extracellular domain leading to a truncation of the protein upstream of the transmembrane domain (Fig. 1B and C). This truncated subunit would not form receptor subunits as no transmembrane regions or pore region would be translated.

Vigabatrin-hypersensitive patients

The vigabatrin-hypersensitive patients were chosen for their clinical response to vigabatrin but had exacerbated hypotonia sedation and/or respiratory difficulties that reverted upon cessation of therapy. These included a patient (case 3) with *de novo GABRB3* variant p.Glu77Lys (Kothur *et al.*, 2018), that was previously reported as part of 105 patients investigated using a gene panel where the detailed case was not previously reported, and a previously reported *de novo GABRB3* variant p.Thr287Ile (Papandreou *et al.*, 2016) with an updated case report (case 4). The p.Glu77Lys and p.Thr287Ile variants were located at the conserved extracellular loop 2 and M2 domains (Fig. 1B–D), respectively that play key roles in channel activation.

Clinical details of vigabatrin-hypersensitive patients

Case 3 (p.Glu77Lys) is a 4-year-old girl who presented with spasms since the age of 5 months in the form of sudden jerking of arms and legs occurring in clusters of 5–10 spasms, with 4–5 clusters per day (Table 1). Her early development prior to spasms was normal, although there was loss of social smile and reduced cooing for 1 month before spasm onset. On examination her head circumference was at 90th centile, weight was 90th centile and length was 75th centile. She was hypotonic with poor neck control, delayed visual maturation and responsiveness. Her EEG showed high amplitude spike and wave and polyspike and wave in the posterior region, and MRI brain showed the prominence of CSF spaces and mild ventriculomegaly. Her CSF studies including neurotransmitters were normal. She was treated with corticosteroid according to UKISS protocol (10 mg prednisolone four times per day) but continued to have spasms up to 60 spasms/day despite treatment with high dose steroids, plus nitrazepam, sodium valproate, zonisamide and pyridoxine. Due to failure to respond, vigabatrin was introduced, but was associated with extreme drowsiness and exacerbation of hypotonia on only 70 mg/kg/day (800 mg BD), and was therefore weaned off over the next few weeks. She was subsequently stabilized and spasms ceased on a combination of nitrazepam and the ketogenic diet. At 18 months of age, she became seizure free except for infrequent myoclonic seizures. Her ongoing EEG showed frequent slowing over the bilateral frontal region but no epileptiform discharges were noted. Following the cessation of spasms, she showed significant improvement in gross motor development. However, she continued to have persistent language delay with limited social interaction suggestive of autism spectrum disorder.

Case 4 (p.Thr287Ile) is a male infant who presented with neonatal hypotonia, then focal tonic seizures from 3 months of age. EEG showed multifocal discharges but not hypsarrhythmia. Introduction of vigabatrin resulted in seizure cessation but caused severe exacerbation of hypotonia, sedation and respiratory difficulties necessitating cessation of vigabatrin. Unfortunately seizures recurred from 5 months of age, and were refractory to carbamazepine, levetiracetam, topiramate, sodium valproate and the ketogenic diet. At last reported follow-up at 3 years and 2 months, he continues to have refractory epilepsy with 10–20 seizures per day of multiple seizure types with behavioural arrest, focal motor, myoclonic jerks and brief tonic seizures. There is global DD with paucity of movements yet anti-gravity movements, some pyramidal signs with brisk reflexes and upgoing plantars, and some vocalizations. There is subtle dysmorphic features and microcephaly (0.4th centile).

Assessing the molecular phenotype of *GABRB3* missense variants

Assessing the function of $GABA_A$ variants is complicated by the fact that variants are typically dominant and synaptic receptors form with a $2\alpha{:}2\beta{:}1\gamma$ stoichiometry. As patients have one normal and one mutated allele, a mixture of receptors with WT and variant subunits will form. For patients carrying a variant in the $\beta3$-subunit ($\beta3^{E77K}$ and $\beta3^{T287I}$), two simple receptor populations express with all WT subunits or with two $\beta3$ variant subunits. These receptors can easily be expressed *in vitro* with free $\gamma2$ and $\alpha1$ subunits, but would be predicted to each only comprise of 25% of the receptor population within the patient (Fig. 2A). The two other receptors expressed contain one WT $\beta3$ and one variant $\beta3$ subunit. For a random distribution of subunits, these receptors will comprise ~50% of the receptor population and cannot easily

Table 1 Clinical phenotypes

	Case 1	Case 2	Case 3 (Kothur *et al.*, 2018)	Case 4 (Papandreou et al., 2016)
Current age (year), sex	2, female	29, female	4, female	3.2, male
Detection method	Multigene epilepsy panel, Sanger confirmation	Sanger	Multigene epilepsy panel, Sanger confirmation	Multigene epilepsy panel, Sanger confirmation
Gene	*GABRB3*	*GABRB3*	*GABRB3*	*GABRB3*
Nucleotide change	c.580C>T	c.580C>T	c.229G > A	c.860C>T
Protein change	p.Arg194*	p.Arg194*	p.Glu77Lys	p.Thr287Ile
Type of variant	Stop	Stop	Missense	Missense
Inheritance	Maternal	N/A	*De novo*	*De novo*
Age of onset epilepsy	7 months	2 years	5 months	3 months
Epilepsy syndrome	Infantile spasms	Atonic seizures	Infantile spasms	Unclassified DEE
Seizure type	Infantile spasms	Atonic seizures	Infantile spasms	Tonic, myoclonic and focal motor seizures
Development	DD	Learning difficulties	Hypotonia, delayed visual maturation	Hypotonia, severe global DD
Other features	Right sided hemiplegia, plagiocephaly		Autistic features	Microcephaly, mild dysmorphism
Interictal EEG findings	Hypsarrhythmia	NA	High amplitude Spike and Wave and poly-spike	High amplitude multifocal discharges
MRI findings	Porencephalic cyst left ACM area with secondary Wallerian degeneration tractus corticospinalis brainstem left: prenatal ischemic insult left ACM area; almost no myelinization left hemisphere (7 months)	NA	Prominence of CSF spaces and mild ventriculomegaly (5 months)	Normal (14 months)
Medication tried	Prednisolone, vigabatrin	Valproic acid	Steroids, vigabatrin, valproate, zonisamide, pyridoxine, ketogenic diet, nitrazepam	Vigabatrin, carbamazepine, topiramate, sodium valproate
Reaction to vigabatrin	Seizure reduction, no side effects	NA	Severe drowsiness and hypotonia	Severe hypotonia, sedation, respiratory difficulties
Ongoing treatment	Valproic acid	None	Nil	Ketogenic diet, levetiracetam
Seizure outcomes	Seizure free by 10 months	Seizure free from 18 years	Infrequent myoclonic seizures, cessation of spasms	Ongoing focal motor, tonic, myoclonic seizures
Developmental outcome	Global DD, speech delay		Severe autism and language delay (few words at 5 years) and hyperactivity	Severe global DD

Did not include GABA peak as this is filtered in routine reporting.

be evaluated by the heterologous expression of free subunits (Fig. 2A).

We recently developed an approach to determine the function of each of these subunit combinations (Absalom *et al.*, 2019) by engineering all five $GABA_A$ receptor subunits into the native receptor arrangement using linkers with unique restriction sites (γ2-β3-α1-β3-α1) (Fig. 2A and B). This approach enables us to generate a library of receptors containing one or two copies of the mutation by a 'cut and paste' approach and then express them individually, recapitulating the full molecular phenotype of the variant. We analyse the function of all possible receptors by performing two-electrode voltage-clamp electrophysiology on concatenated WT, one copy or two copies of the $\beta3^{E77K}$ and $\beta3^{T287I}$ mutations expressed in *Xenopus* oocytes.

$\beta3^{E77K}$ and $\beta3^{T287I}$ variants do not alter maximal GABA-evoked current amplitudes

Using this approach we developed single and double mutated receptor constructs from the original WT construct (γ2-β3-α1-β3-α1) for each variant. This totalled six unique receptor constructs and mRNA was synthesized for each construct and injected into *Xenopus* oocytes. All three receptor constructs for each variants expressed robustly with I_{3mM_GABA}-evoked currents in the 0.9–2.2 µA range (Fig. 2C). No significant difference in the maximum currents elicited by 3 mM GABA were observed between all six receptor constructs [one-way ANOVA, $F(6,111) = 2.062$, $P = 0.0633$; Table 2]. While not significantly different, the γ2-$\beta3^{E77K}$-α1-$\beta3^{E77K}$-α1 receptor

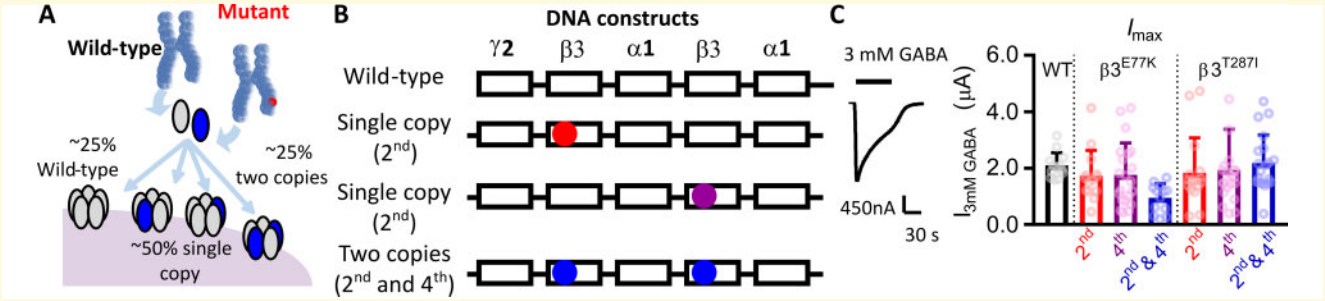

Figure 2 Design and expression levels of synaptic receptor constructs. (**A**) Diagram depicting the mixture of receptors formed on the cell surface from a *de novo* variant. Assuming equivalent expression and random assembly, four different receptors will be expressed at equal ratios. (**B**) Concatenated DNA constructs used to determine the functional effect of each variant at all expressed receptors. Five subunits were linked in the order γ2-β3-α1-β3-α1 such that cRNA injected into *Xenopus* oocytes resulted in pentameric receptors of the same orientation as synaptic receptors. Three separate constructs were created for the $\beta3^{E77K}$ and $\beta3^{T287I}$ variants where the variant was introduced into the 2nd subunit (red), the 4th subunit (purple) or both the 2nd and 4th subunits (blue) of the construct. This replicated the effect of the variant *in vivo*, where a WT receptor, two receptors containing a single copy of the variant and a receptor containing two copies of the variant are expressed. (**C**) Representative trace from two-electrode voltage recordings of a response to 3 mM GABA (black bars) of *Xenopus* oocytes injected with the WT concatenated receptor construct. (**D**) Bar graph of maximum currents elicited by 3 mM GABA at receptors (black) and at receptors containing $\beta3^{E77K}$ or $\beta3^{T287I}$ variants with one copy of the variant in the 2nd subunit (red), one copy in the 4th subunit (purple) and two copies in the 2nd and 4th subunit (blue). Dots represent individual experiments and bars represent mean ± SD.

had approximately a 2-fold reduction in maximum current that may arguably be a result of a reduced maximum open probability, reduced cell surface expression or impaired protein folding. However, as the single subunit $\beta3^{E77K}$ variant receptors exhibited similar absolute currents to the WT, it is unlikely that such a minor change in a 25% receptor subpopulation has much overall effect in a patient.

$\beta3^{E77K}$ and $\beta3^{T287I}$ variants increases the potency of GABA

$GABA_A$ receptors are activated by GABA in a concentration-dependent manner, where a reduction in GABA potency has commonly been attributed to loss-of-function *GABRB3* variants (Janve *et al.*, 2016; Møller *et al.*, 2017). The $\beta3^{E77}$ residue is located in loop 2, part of the 'coupling domain' incorporating loops two, seven and nine, the pre-M1 helix and the M2 and M3 loop, that alters conformation during channel activation (Fig. 3A) (Kash *et al.*, 2004; Laverty *et al.*, 2019). Therefore, to determine if the GABA-activation properties of synaptic receptors were altered by the $\beta3^{E77K}$ variant, we estimated the maximal open probability and constructed concentration–response curves of receptors to GABA.

The potency of GABA at the WT γ-β3-α1-β3-α1 receptor construct was 69 μM and the maximum estimated open probability 0.94 (Fig. 3B–D). With observed values in the 0.93-1.0 range, none of the receptors containing the $\beta3^{E77K}$ variant altered the maximum estimated open probability [one-way ANOVA, $F(6,62) = 1.17$, $P = 0.34$; Table 2]. In contrast, there was a significant difference in the GABA potency at the three different receptors [one-way ANOVA, $F(6,67) = 6.208$ $P < 0.0001$ $logEC_{50}$].

Receptors with one copy of the $\beta3^{E77K}$ variant significantly increased the GABA potency with EC_{50}'s ranging between 20-34 μM for γ-$\beta3^{E77K}$-α1-β3-α1 and γ-β3-α1-$\beta3^{E77K}$-α1 ($P < 0.01$ Dunnett's *post hoc* test; $logEC_{50}$ c.f. WT; Table 2). Receptors with two copies of the $\beta3^{E77K}$ variant also displayed a significant increase in the GABA potency compared to WT, reducing the EC_{50} to 21 μM (Table 2).

The $\beta3^{T287}$ residue is located in the M2 region that lines the channel pore, lying one turn of the helix above a key leucine conserved across ligand-gated ion channels that forms a narrow diameter within the pore (Phulera *et al.*, 2018; Laverty *et al.*, 2019) (Fig. 4A). The M2 helix undergoes a tilt when the receptor transitions to an open state, and as such we estimated the maximal open probability and constructed concentration–response curves of $\beta3^{T287I}$ concatenated receptors to GABA.

None of the receptors containing $\beta3^{T287I}$ variants altered the Est Po_{max} with values ranging between 0.93 and 1.0 [one-way ANOVA, $F(6,62) = 1.17$, $P = 0.34$; Fig. 4B; Table 2]. Receptors with one copy of the variant either significantly increased the GABA potency, reducing the EC_{50} to 23 μM for γ-β3-α1-$\beta3^{T287I}$-α1, $P < 0.01$ Dunnett's *post hoc* test; $logEC_{50}$ c.f. WT or the increase was not significant (EC_{50} = 43 μM for γ-$\beta3^{T287I}$-α1-β3-α1, $P > 0.05$; Dunnett's *post hoc* test; Fig. 4C and D; Table 2). Receptors with two copies of the $\beta3^{T287I}$ variants displayed significant increase in the GABA potency compared to WT, reducing the EC_{50} to 22 μM ($P < 0.01$, Dunnett's *post hoc* test; Fig. 4C and D, Table 2).

Thus, the common molecular phenotype for the vigabatrin-hypersensitive variants that we identified in receptors containing the $\beta3^{E77K}$ or the $\beta3^{T287I}$ variant is an increase in the GABA potency, and therefore an increase in

Table 2 Functional parameters of receptors containing one, or two, copies of each variant

β3 Variants	Construct	Activation properties		
		$I_{3mM\ GABA}$ ± SEM (nA)	EC_{50} (μM)−log_{EC50} ± SEM	Est Po
WT[a]	γ2-β3-α1-β3-α1	2095 ± 126 (13)[b]	69 (14) 4.11 ± 0.06	0.94 ± 0.03 (10)
	γ2-β3-α5-β3-α5	808 ± 90 (20)	108 (10) 3.93 ± 0.05	0.90 ± 0.01 (10)
$β3^{E77K}$	γ2-$β3^{E77K}$-α1-β3-α1	1731 ± 241 (21)	20 (10) 4.62** ± 0.07	0.98 ± 0.04 (10)
	γ2-β3-α1-$β3^{E77K}$-α1	1764 ± 245 (13)	27 (10) 4.63** ± 0.06	1.02 ± 0.04 (10)
	γ2-$β3^{E77K}$-α1-$β3^{E77K}$-α1	946 ± 140 (16)	21 (10) 4.69** ± 0.06	0.94 ± 0.04 (8)
	γ2-$β3^{E77K}$-α5-$β3^{E77K}$-α5	465 ± 66 (20)	49 (10) 4.31*** ± 0.04	0.95 ± 0.05 (10)
$β3^{T287I}$	γ2-$β3^{T287I}$-α1-β3-α1	1838 ± 310 (21)	43 (10) 4.36 ± 0.08	0.97 ± 0.02 (10)
	γ2-β3-α1-$β3^{T287I}$-α1	1936 ± 316 (20)	23 (10) 4.62** ± 0.12	0.93 ± 0.01 (11)
	γ2-$β3^{T287I}$-α1-$β3^{T287I}$-α1	2181 ± 223 (14)	22 (10) 4.65** ± 0.06	1.00 ± 0.02 (10)
	γ2-$β3^{T287I}$-α5-$β3^{T287I}$-α5	712 ± 13 (20)	45 (10) 4.30*** ± 0.08	1.01* ± 0.03 (10)

[a]WT values except rate constants are also reported in Absalom *et al.* (2019).
[b]Number of individual oocytes (*n*) are in parentheses.
*$P < 0.05$.
**$P < 0.01$.
***$P < 0.001$, one-way ANOVA, Dunnett's *t*-test c.f. WT.

the activation of the receptors at lower GABA concentrations. This contrasts from previous findings that variants in *β3* subunits typically result in loss-of-function receptors. However, variants may have other characteristics that would lead to loss in inhibitory GABAergic transmission and thus we next investigated desensitization profiles that have been reported to have changed in other $GABA_A$ receptor subunit variants (Butler *et al.*, 2018).

$β3^{E77K}$ and $β3^{T287I}$ variants do not alter macroscopic desensitization characteristics of the receptors

Upon activation by GABA, the channel pore of the $GABA_A$ receptor opens, then shifts to an equilibrium that includes a desensitized state that is unable to conduct ions. In the case of $GABA_A$ receptors, chloride passes from the outside to the inside of the cell to hyperpolarize the cell, acting as a 'brake' for neuronal firing. If the receptor is highly desensitized the required chloride is unable to pass through the receptor and neuronal firing continues. Conversely, if the receptor does not desensitize then chloride will continue to permeate for extended times and neuronal firing could be excessively reduced. Variants in $GABA_A$ receptor subunits have previously been identified that increase the desensitization properties of the receptor (Shen *et al.*, 2017; Butler *et al.*, 2018) leading to an overall loss-of-function profile.

To quantify the macroscopic desensitization, we applied a single concentration of GABA, fitted the current decay to an exponential curve and determined the rate constant at different concentrations of GABA (Fig. 5A–C). As the potency of receptors with two copies of the variant was altered the most, we performed these experiments only at receptors containing two copies of the variants where any change in desensitization would be the largest. For WT receptors, the rate constants at concentrations of 0.1, 0.3, 1 and 3 mM GABA were 11 ± 2 ms, 22 ± 2 ms, 28 ± 2 ms and 31 ± 2 ms, for the $β3^{E77K}$ were 30 ± 4 ms, 42 ± 3 ms, 56 ± 5 ms and 47 ± 6 ms and for the $β3^{T287I}$ receptors were 20 ± 3 ms, 30 ± 6 ms, 28 ± 6 ms and 36 ± 6 ms ($n = 6$).

To compare the rate constants between receptors, we plotted decay constants as a function of the log_{10} GABA concentration. Empirically, the data fitted well to a linear curve (Fig. 5D and E). An *F*-test demonstrated that the WT and $β3^{T287I}$ linear functions could be described by the same curve [$F(2,45) = 2.34$, $P = 0.0108$], but the WT and $β3^{E77K}$ linear functions could be described by different curves [*F*-test, $F(2,51) = 28.09$, $P < 0.001$]. A further Mann–Whitney test demonstrated that the WT and $β3^{E77K}$ data were not significantly different ($P = 0.111$). This demonstrates that the variants do not lead to a loss-of-function molecular phenotypes through alterations in the desensitization profiles.

Taken together, these data demonstrate that both the $β3^{E77K}$ and $β3^{T287I}$ variants result in a significant increase

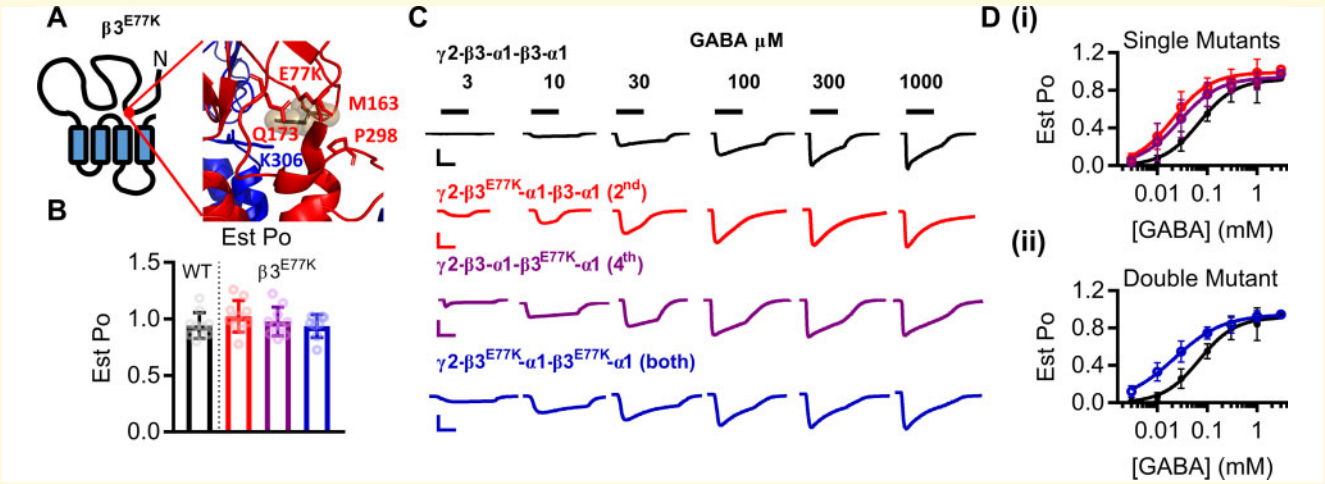

Figure 3 Gain-of-function molecular phenotype of $\beta3^{E77K}$ variant. (**A**) The location of the $\beta3^{E77K}$ variant in a schematic of the β3 subunit and in the protein structure displaying a close-up of the coupling interface between the extracellular and transmembrane regions. (**B**) Bar graphs representing individual experiments (dots) and the mean ± SD for the estimated open probability of WT (black) and $\beta3^{E77K}$ constructs containing one copy of the variant in the 2nd subunit (red), one copy in the 4th subunit (purple) and two copies in the 2nd and 4th subunit (blue). The estimated open probability was calculated by comparing the response at 3 mM GABA to the response at 10 mM GABA, 3 μM etomidate and 1 μM diazepam. (**C**) Representative traces of currents recorded from *Xenopus* oocytes injected with WT (black) and $\beta3^{E77K}$ constructs containing one copy of the variant in the 2nd subunit (red), one copy in the 4th subunit (purple) and two copies in the 2nd and 4th subunit (blue). GABA concentrations were applied as indicated by the black bars to construct the concentration–response curves. Scale bars indicate 200 nA and 30 s, except for the blue bar that represents 50 nA and 30 s. (**D**) Concentration–response curves of WT and (i) concatenated constructs containing the $\beta3^{E77K}$ variant in the 2nd (red) or 4th subunit and (ii) the concatenated construct containing a $\beta3^{E77K}$ variant in the 2nd and 4th subunits. Symbols represent mean ± SD and data were fitted to the Hill equation.

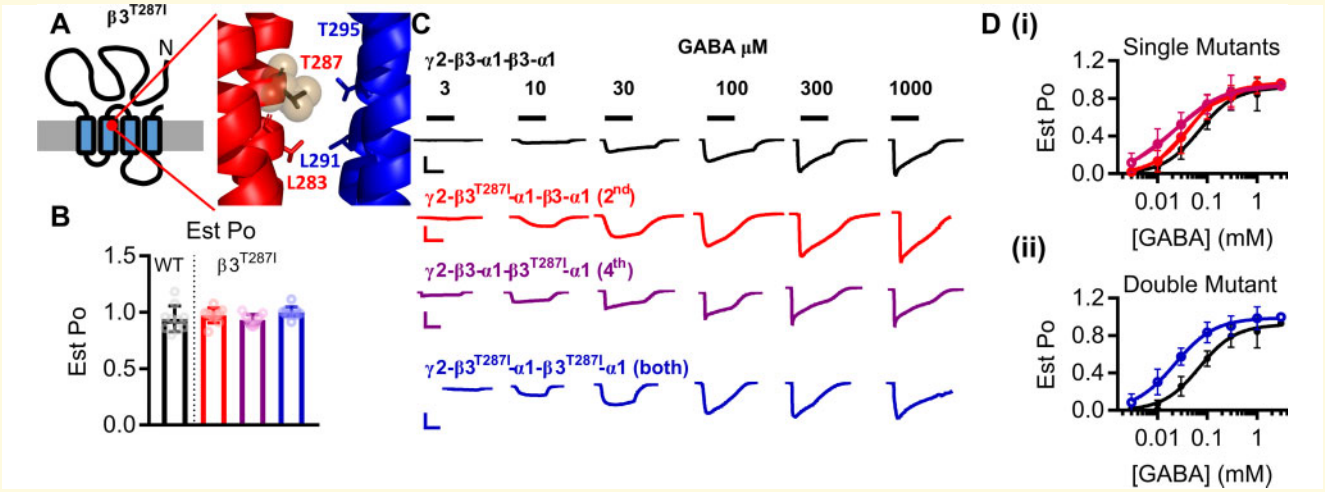

Figure 4 Gain-of-function molecular phenotype of $\beta3^{T287I}$ variant. (**A**) The location of the $\beta3^{T287I}$ variant in a schematic of the β3 subunit and in the protein structure displaying a close-up of the M2 domains of the β3 (red) and α1 (blue) subunits. (**B**) Bar graphs representing individual experiments (dots) and the mean ± SD for the estimated open probability of WT (black) and $\beta3^{T287I}$ constructs containing one copy of the variant in the 2nd subunit (red), one copy in the 4th subunit (purple) and two copies in the 2nd and 4th subunit (blue). The estimated open probability was calculated by comparing the response at 3 mM GABA to the response at 10 mM GABA, 3 μM etomidate and 1 μM diazepam. (**C**) Representative traces of currents recorded from *Xenopus* oocytes injected with WT (black) and $\beta3^{T287I}$ constructs containing one copy of the variant in the 2nd subunit (red), one copy in the 4th subunit (purple) and two copies in the 2nd and 4th subunit (blue). GABA concentrations were applied as indicated by the black bars to construct the concentration–response curves. Scale bars indicate 200 nA and 30 s, except for the purple bar that represents 2 000 nA and 30 s. (**D**) Concentration–response curves of WT and (i) concatenated constructs containing the $\beta3^{T287I}$ variant in the 2nd (red) or 4th subunit and (ii) the concatenated construct containing a $\beta3^{T287I}$ variant in the 2nd and 4th subunits. Symbols represent mean ± SD and data were fitted to the Hill equation.

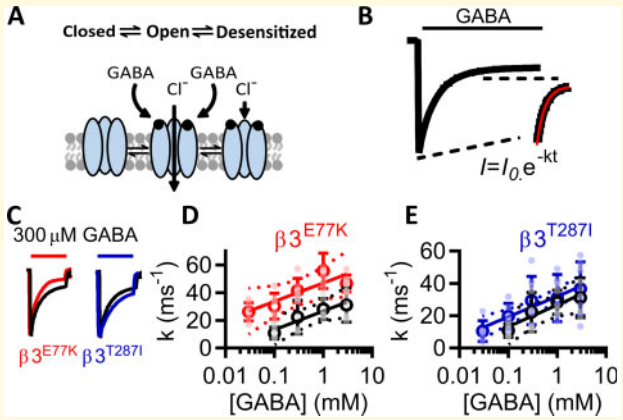

Figure 5 Desensitization properties of $\beta3^{E77K}$ and $\beta3^{T287I}$ variants. (**A**) Schematic displaying desensitization of the receptor, whereby subsequent to GABA binding, $GABA_A$ receptors shift between open and closed desensitizing states. (**B**) To measure the rate of desensitization, the recording apparatus was configured to remove dead volume and GABA was applied for 120 s, and the deactivation rates in the presence of GABA were fitted to an exponential decay function, with the deactivation constant determined for different GABA concentrations against WT and double mutant receptors. (**C**) Comparison of the WT and double mutant $\beta3^{E77K}$ and $\beta3^{T287I}$ receptors. Traces normalized to the peak current are shown for responses to 300 µM GABA at WT (black), $\beta3^{E77K}$ (red) and $\beta3^{T287I}$ receptors (blue) receptors, with the scale bar indicating 50 s. (**D**) and (**E**) Deactivation constants were plotted against the log of GABA concentrations and fitted to a linear function (95% confidence interval in dotted line) for the WT (black) and (**D**) $\beta3^{E77K}$ (red) and (**E**) $\beta3^{T287I}$ receptors (blue) receptors.

in the sensitivity of the receptor to GABA without increased desensitization, consistent with a gain-of-function molecular phenotype.

Response of $\beta3^{E77K}$ and $\beta3^{T287I}$ variants to nitrazepam

Benzodiazepines, including nitrazepam, are positive allosteric modulators of $GABA_A$ receptors that predominately affect phasic currents, usually through prolonging inhibitory postsynaptic currents (Otis and Mody, 1992). As nitrazepam reduced seizures without adverse effects for the patient with the $\beta3^{E77K}$ variant, we evaluated the sensitivity of receptors to nitrazepam and compared the potency and efficacy of nitrazepam modulation of GABA (EC_{10})-elicited currents (1 µM) at WT and variant receptors.

We constructed concentration–response curves to nitrazepam at WT receptors and receptors containing two copies of the $\beta3^{E77K}$ or $\beta3^{T287I}$ variant. The WT receptor had an EC_{50} of 122 µM ($-\log EC_{50} = 6.96 \pm 0.03$) to nitrazepam and a maximum modulation (E_{max}) of $186 \pm 4.6\%$. ($n = 6$) (Fig. 6A). Neither the $\beta3^{E77K}$ and $\beta3^{T287I}$ variant significantly altered the potency of nitrazepam with EC_{50}'s of 99 and 89 nM, respectively [$-\log EC_{50} = 7.04 \pm 0.03$ and 7.05 ± 0.02, $n = 5$, one-way ANOVA, $F(3,17) = 3.258$ $P > 0.05$]. The efficacy of nitrazepam was significantly reduced to 122% at $\beta3^{E77K}$ [one-way ANOVA, $F(3,16) = 61.9$, $P < 0.0001$] ($E_{max} = 122 \pm 3\%$, $n = 5$, Dunnett's *post hoc* test, $P < 0.0001$) but not at $\beta3^{T287I}$ receptors ($E_{max} = 174 \pm 4.7\%$, $n = 5$, Dunnett's *post hoc* test, $P > 0.05$). These data suggest that nitrazepam is less efficacious at modulating receptors containing a $\beta3^{E77K}$ variant, likely exerting greater effects in the patient via WT receptor subtypes.

$\beta3^{E77K}$ and $\beta3^{T287I}$ variants increase GABA potency of extrasynaptic α5-containing receptors

$\beta3$ subunits are incorporated into a variety of $GABA_A$ receptors, including extrasynaptic $\alpha5\beta3\gamma$ receptors that mediate tonic currents. To determine how the $\beta3^{E77K}$ and $\beta3^{T287I}$ variants affected these receptors, we created a $\gamma2$-$\beta3$-$\alpha5$-$\beta3$-$\alpha5$ WT, $\gamma2$-$\beta3^{E77K}$-$\alpha5$-$\beta3^{E77K}$-$\alpha5$ and $\gamma2$-$\beta3^{T287I}$-$\alpha5$-$\beta3^{T287I}$-$\alpha5$ constructs. mRNA was synthesized for each construct and injected into *Xenopus* oocytes. All three receptor constructs expressed robustly with I_{3mM_GABA}-evoked currents in the 0.5–0.8 µA range (Fig. 6B). No significant difference in the maximum currents elicited by 3 mM GABA were observed for the variants [one-way ANOVA, $F(2,59) = 3.004$, $P = 0.0571$; Table 2], although similar to the α1 constructs the $\gamma2$-$\beta3^{E77K}$-$\alpha5$-$\beta3^{E77K}$-$\alpha5$ receptor had the lowest absolute currents.

The potency of GABA at the WT γ-$\beta3$-$\alpha5$-$\beta3$-$\alpha5$ receptor construct was 108 µM and an Est P_{Omax} value of 0.90 (Fig. 6C and D). The Est P_{Omax} values were in a range of 0.90–1.01 and no significant difference was observed [one-way ANOVA, $F(2,27) = 2.867$, $P = 0.07$; Table 2]. However, both variants significantly reduced the GABA potency by ~2-fold compared to WT [one-way ANOVA, $F(2,27) = 15.37$ $P < 0.0001$ $\log EC_{50}$, $P < 0.0001$]. Taken together, these data demonstrate that both the $\beta3^{E77K}$ and $\beta3^{T287I}$ variants result in a significant increase in the sensitivity of the receptor to GABA without increased desensitization, consistent with a gain-of-function molecular phenotype. This is the same functional change occurring in $\alpha5\beta3\gamma2$ extrasynaptic receptor as is occurring when $\beta3^{E77K}$ and $\beta3^{T287I}$ variants are incorporated into the $\alpha1\beta3\gamma2$ synaptic receptor.

Why would gain of function variants lead to vigabatrin hypersensitivity?

Vigabatrin is an irreversible inhibitor of GABA transaminase that blocks intracellular GABA degradation at the presynaptic terminal. The increased intracellular GABA concentrations reverse the direction of GABA transport, leading to non-vesicular release of GABA into the extracellular space (Wu *et al.*, 2001, 2003) (Fig. 6E). In hippocampal cultures, 4 days of vigabatrin exposure

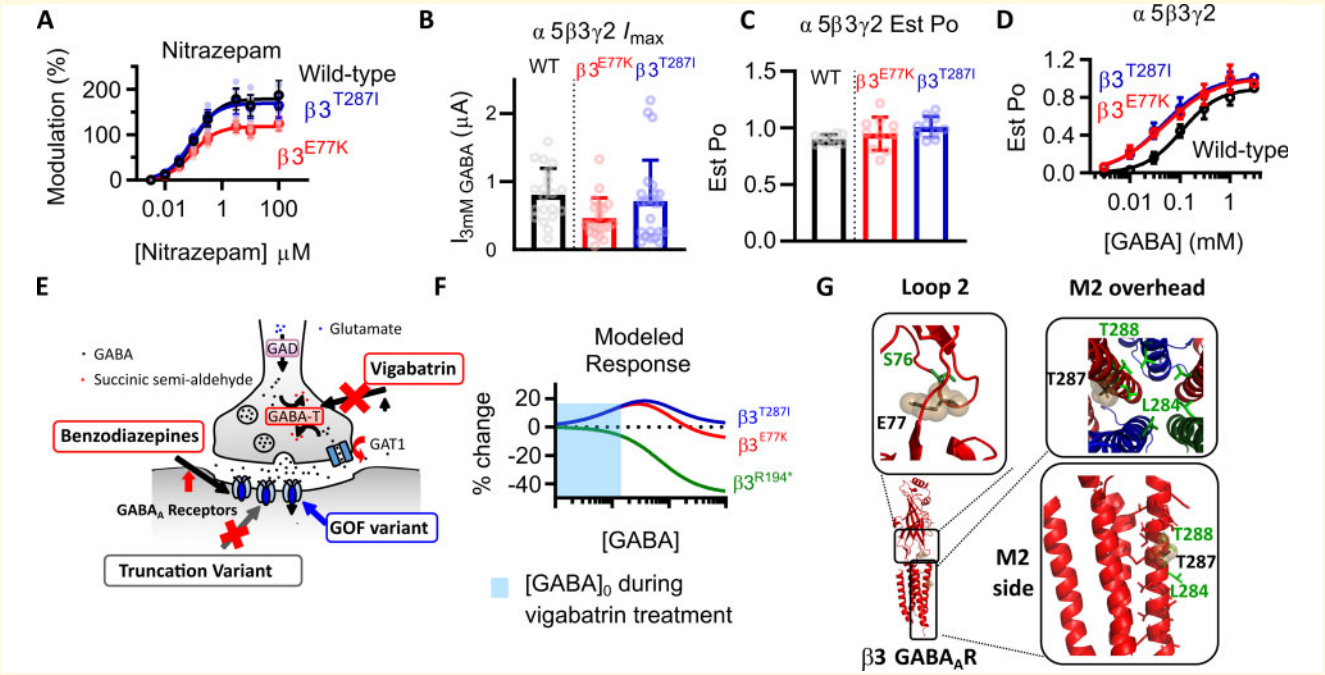

Figure 6 Vigabatrin and $GABA_A$ receptor variants at receptors mediating tonic currents. (**A**) Concentration–response curves of the positive modulation of EC_{10} GABA currents by nitrazepam at WT (black), $\beta3^{E77K}$ (red) and $\beta3^{T287I}$ (blue) receptors The maximum modulation was significantly reduced at $\beta3^{E77K}$ receptors compared to WT ($P < 0.01$, one-way ANOVA with Dunnett's *post hoc* test). (**B**) Bar graph of maximum currents elicited by 3 mM GABA at WT γ2-β3-α5-β3-α5 receptors (black) and receptors containing two copies of the $\beta3^{E77K}$ (red) or $\beta3^{T287I}$ (blue). Dots represent individual experiments and bars represent mean ± SD. (**C**) Bar graphs representing individual experiments (dots) and the mean ± SD for the estimated open probability of WT γ2-β3-α5-β3-α5 (black) $\beta3^{E77K}$ (red) or $\beta3^{T287I}$ (blue) receptors. The estimated open probability was calculated by comparing the response of 3 mM GABA was compared to the response to 10 mM GABA and 10 μM etomidate. (**D**) Concentration–response curves of WT γ2-β3-α5-β3-α5 (black) $\beta3^{E77K}$ (red) or $\beta3^{T287I}$ (blue) receptors to GABA. Symbols represent mean ± SD and data were fitted to the Hill equation. (**E**) Depiction of an inhibitory synapse describing the mechanism of action of vigabatrin. GABA transaminase catalyses the breakdown of GABA into succinic semi-aldehyde, which is inhibited by vigabatrin. This reverses the transport gradient of GAT-1, leading to non-vesicular release of GABA into the synapse to increases the tonic current of the post-synaptic neuron. In two patients with hypersensitivity to vigabatrin, a variant was identified in the β3 subunit of the $GABA_A$ receptor that increased the response of the receptor to vigabatrin, while the patients with a truncation of the *GABRB3* gene that causes a loss-of-function variant, responded to vigabatrin without hypersensitivity. (**F**) Modelled change in response compared to the WT of $\beta3^{E77K}$ (red) and $\beta3^{T287I}$ receptors (blue) compared to the WT, showing the predicted difference in current levels at different GABA concentrations. The *x*-axis indicates no change. The shaded region is the expected $[GABA]_0$ concentration elicited by vigabatrin. (**G**) Structure of the α1β3γ2 $GABA_A$ receptor (Masiulis *et al.*, 2019) showing the location of the $\beta3^{E77}$ residue within loop 2 (black sticks and spheres) and the $\beta3^{S76}$ residue that is homologous to the A52 residue of the GlyR that is associated with hyperekplexia (Plested *et al.*, 2007). The $\beta3^{T287}$ residue is shown in a side and overhead view of the M2 region (black sticks and spheres). Also shown is the central $\beta3^{L284}$ and $\beta3^{T288}$ residue that is also associated with DEE (Hernandez *et al.*, 2017).

caused an average increase in neuronal inhibition of 9 nS, with an implied $[GABA]_0$ of 0.5 μM. This results in large increases in tonic currents of the postsynaptic cell with little to no decrease in phasic inhibitory currents (Wu *et al.*, 2003).

The $\beta3^{R194*}$ reduces the chloride flux at all GABA concentrations and, due to the reduction in functional receptors, the tonic current induced by vigabatrin likely would be lower than the WT. In contrast, the population of receptors expressed by both the $\beta3^{E77K}$ and $\beta3^{T287I}$ increased the chloride flux at lower GABA concentrations. The expression of concatenated $GABA_A$ receptors in oocytes leads to a 30-fold higher GABA EC_{50} than in recombinant mammalian cells, where the $EC_{50} \sim 2\,\mu$M (Mortensen *et al.*, 2011). Therefore, at GABA concentrations in the oocytes equivalent to the $[GABA]_0$ (~15 μM), we record the highest increases in current elicited at receptors containing the $\beta3^{E77K}$ and $\beta3^{T287I}$ variants compared to WT, with ~20% increase in currents. Vigabatrin, through the reversal of GABA transport in the presynaptic neuron, would therefore likely lead to considerably increased tonic inhibition in these variants compared to the WT receptor. Benzodiazepines, that do not elicit phasic currents from synaptic receptors, are unlikely to lead to the same adverse effect.

Discussion

$GABA_A$ receptors are the primary mediators of inhibitory neurotransmission in the developing and adult brain. Variants in $GABA_A$ receptors that alter the function of the receptor can modify neuronal excitability, leading to neurodevelopment disorders including epilepsy. Pathogenic variants in *GABRB3* are commonly identified in individuals with mild to severe forms of epilepsy (Janve *et al.*, 2016; Møller *et al.*, 2017), signifying the importance of this gene in brain development and function. Located within an imprinting region that spans the 15q11-13 chromosome, variants in the *GABRB3* gene are often clustered around central functional domains such as the extracellular GABA binding site, transmembrane helixes supporting or lining the pore (M1 and M2) or loop regions that couple ligand binding to channel gating (Niturad *et al.*, 2017). We, and others, have shown that variants in $GABA_A$ receptors often result in loss of receptor function predominantly manifesting as mutations that reduce receptor function by impairing channel gating or as a result of reduced subunit expression due to impaired transcription, impaired translation, misfolding and degradation, truncation, endoplasmic reticulum retention (Janve *et al.*, 2016; Møller *et al.*, 2017; Absalom *et al.*, 2019; Hernandez and Macdonald, 2019; Hernandez *et al.*, 2019).

Both the $\beta3^{E77}$ and $\beta3^{T287}$ residues are located in key activation regions of the receptor within loop 2 and the pore-lining transmembrane domain (M2) of the subunit, respectively. Loop 2 alters conformation during receptor activation, whereby the M2 region tilts to convert the channel from closed to open state (Laverty *et al.*, 2019; Masiulis *et al.*, 2019). Variants in these structural regions have been identified in $GABA_A$ receptor subunits, and other ligand-gated ion channels, that lead to genetic disorders with both loss- and gain-of-function variants being reported for the different ion channels (Fig. 6E) (Plested *et al.*, 2007). The $\beta3^{T287I}$ variant at the 13′ position faces the adjacent M2 domain of the neighbouring subunit, as opposed to the ion pore itself (Fig. 6E), and with a homologous variant identified in the *GABRB1* gene (p.Thr287Ile), albeit with no functional data (Lien *et al.*, 2016), the location appears to be a hotspot for spontaneous mutations. Alternatively, an evaluation of the $\beta2$ glutamate to lysine variant homologous to $\beta3^{E77K}$ showed no change in either the maximum absolute currents of GABA or concentration–response curve (Kash *et al.*, 2004). For variants in these regions, it appears essential to perform functional genomics to ascertain the molecular phenotype of the variant.

The structural location of the variants may also underlie the differences in the sensitivities to nitrazepam. The $\beta3^{E77}$ residue within loop 2 couples to the M2-M3 loop to mediate transitions earlier in the activation process than the M2 region where the $\beta3^{T287}$ residue is located. The difference between nitrazepam efficacy in these two variants is most likely due to $\beta3^{E77K}$ altering the equilibrium between pre-activated conformational states of the receptor that benzodiazepines also alter (Gielen *et al.*, 2012). In contrast, $\beta3^{T287I}$, within the M2 region, is more likely to alter the equilibrium between conformational states later in the activation process, perhaps even between closed and open states, leading to little to no change in the efficacy of nitrazepam.

In this study, we describe four individuals with epilepsy and DD, three of which were prescribed and had different reactions to the anti-epileptic drug vigabatrin. One patient had a truncation within the *GABRB3* gene that introduces a stop codon in the DNA coding sequence upstream of the transmembrane regions ($\beta3^{R194*}$ truncation). This truncation would abolish the functional expression of the $\beta3$ subunit, a classical loss-of-function variant. Interestingly this patient had worsening seizures in response to oxcarbazepine, a sodium channel blocker. Oxcarbazepine inhibits GABA release from the presynaptic terminal initiated via presynaptic $Na_V1.1$ channels. As this patient has a typical loss-of-function *GABRB3* variant, the addition of oxcarbazepine would further reduce the GABA-mediated inhibitory currents that are already lower than normal. This adverse response could have been avoided if the genetic information was known prior to treatment. In contrast this patient responded well to vigabatrin with reduced seizure frequency, becoming seizure free at 12 months as vigabatrin enhances GABA-mediated inhibitory currents.

In this patient, vigabatrin would be expected to increase the levels of tonic inhibition through the non-vesicular release of GABA mediated via the reversal of GABA transport induced by the blockade of GABA transaminase. $GABA_A$ receptors at the synapse are now persistently activated by the increased GABA concentrations, whereby these receptors will be continually activated leading to excess tonic currents. As a means to alleviate seizures that are ultimately caused by reduced $GABA_A$ receptor expression, increased tonic inhibition is already known to be a key compensatory mechanism responsible for the relatively mild phenotype of mice with homozygous $\alpha1$ $GABA_A$ receptor deletions. Apart from a slight handling tremor, these mice have no pronounced phenotype, and analysis of tonic currents at cerebral granular cells identified ~60% increases in tonic current, identifying a plausible compensatory mechanism (Ortinski *et al.*, 2006). Utilizing vigabatrin to increase the tonic current in patients with *GABRB3* truncation variants would thus represent a rational approach to therapy.

The two patients carrying the heterozygous missense *GABRB3* variants (p.Glu77Lys and p.Thr287Ile) initially showed a promising reduction in seizures to vigabatrin, but subsequently deteriorated with decreased alertness, extreme drowsiness, hypotonia, sedation and respiratory difficulties. These patients exhibited an atypical gain-of-function molecular phenotype as evidenced by increased GABA sensitivity, no alterations to receptor

desensitization characteristics, and little change to the Est open probability or maximum GABA currents. The enhanced sensitivity to GABA at $\beta3^{E77K}$ and $\beta3^{T287I}$ containing receptors is likely to underlie the hypersensitive clinical reaction to vigabatrin. The increase in non-vesicular GABA release that is converted to a tonic current will be exacerbated at receptors containing variants that increase the potency of GABA. Furthermore, when the $\beta3^{E77K}$ or $\beta3^{T287I}$ variants are incorporated into $\alpha5\beta3\gamma2$ receptors that normally mediate tonic currents, the resulting receptors also display increased GABA sensitivity. Under vigabatrin treatment, any compensation mechanisms appear unable to prevent the hypersensitive reactions in these two patients with *GABRB3* variants that result in gain-of-function molecular phenotypes. Despite good efficacy for treating infantile spasms, including our case 1, ~5% of patients exhibit symptoms of vigabatrin hypersensitivity manifesting as significant drowsiness, hypotonia and respiratory difficulties (Lux *et al.*, 2005), and similarly to what was observed with our patients, the adverse response was reversible (Lux *et al.*, 2005; Hernàndez Vega et al., 2014).

Benzodiazepines, however, did not exacerbate symptoms or lead to severe adverse reactions, despite having a mechanism of action that increases GABAergic inhibitory currents. Our patient that carried the $\beta3^{E77K}$ (case 3) variant had a significant reduction in seizures over a 6-month period when treated with nitrazepam combined with a ketogenic diet with no overt adverse response. When nitrazepam was analysed, it had reduced efficacy at this variant but maintains normal efficacy at WT. Furthermore, benzodiazepines act differently to vigabatrin. They are positive allosteric modulators of synaptic $GABA_A$ receptors that selectively bind to α-$\gamma2$ subunit interfaces, mainly prolonging phasic currents rather than increasing tonic currents (Sigel and Ernst, 2018). These results indicate that functional assessment of direct acting $GABA_A$ receptor antiepileptics is important in understanding the mechanism for how patients with distinct $GABA_A$ variants may respond to certain drugs or drug classes.

Gain-of-function variants in *GABRB3* gene have never been previously reported, although a report of gain-of-function variants causing spontaneous GABA ion channel opening and increased GABA potency of recombinant receptors containing the *GABRB1* (p.Leu285Arg) variant located within the M2 domain were associated with alcohol dependence in mice (Anstee *et al.*, 2013). Furthermore enhanced GABA potency has been reported for a variant in the *GABRA5* variant (p.Val294Leu), three in *GABRA3* and one in *GABRA1*. However unlike the $\beta3^{E77K}$ and $\beta3^{T287I}$ variants, these variants apparently either resulted in greater receptor desensitization (Butler *et al.*, 2018; Steudle *et al.*, 2020) or exhibited significantly reduced current amplitudes (Niturad *et al.*, 2017), indicating a possible net loss of GABAergic neurotransmission. The peak concentration of GABA in the synaptic cleft will reach ~1 mM, a saturating GABA concentration. However, this concentration only lasts for less than a millisecond before the GABA is taken up by presynaptic transporters whereby the binding occupancy of $GABA_A$ receptors are not always saturated (Nusser *et al.*, 1997). It would therefore be predicted that in the patients there will be either an increase in the peak amplitude of IPSCs, or a prolonged response of IPSCs, depending on the cell type and synaptic properties in different regions of the brain. Regardless, we would expect a generalized increase in inhibitory GABAergic neurotransmission within these patients.

The idea that increased GABAergic function causes DEE may seem counterintuitive, but extracellular GABA *per se* can have a pro-convulsive action on the epileptic network through disinhibition and alterations in neuronal development (Pavlov and Walker, 2013). Epilepsy-causing loss-of-function variants in the gene encoding the GABA uptake transporter *SLC6A1* result in an accumulation of GABA in the synapses that leads to over activation of synaptic and extrasynaptic $GABA_A$ receptors (Mattison *et al.*, 2018). Furthermore, the *GABRB3* variants described here (p.Glu77Lys and p.Thr287Ile) are *de novo* and manifest during embryonic development. During development, GABA is excitatory and depolarizing, controlling cell proliferation, growth, migration and differentiation via extrasynaptic GABAergic signalling. Thus increased GABA potency at extrasynaptic receptors will affect development and the formation of normal neuronal networks. As the *GABRB3* gene has been associated with epilepsy, development, motor, learning and memory (Tanaka *et al.*, 2012) and autism (Delahanty et al., 2011) and given its location throughout the brain, the gain-of-function molecular phenotype is likely contributing to the clinical presentations of seizures, head lag, autism and DD.

Treatments for patients with gain-of-function mutations must differ to those with loss-of-function mutations since further enhancing 'hyperactive' $GABA_A$ receptors could potentially worsen symptoms. Indeed a patient carrying the *GABRA5* variant that had a gain-of-function phenotype experienced increased seizure frequency while on phenobarbital, and extreme sedation while on clonazepam, albeit this could also be the natural course of the patient's epilepsy (Butler *et al.*, 2018). Evidently, caution must be taken when interpreting why a patient with a specific variant responds differently to one drug than another. Even without background genetic effects, the pharmacodynamics will be complex where both variant and WT receptors will be affected by the drug.

In conclusion, this is the first study that describes $GABA_A$ receptor variants that exhibit a gain-of-function molecular phenotype and may be a hitherto underacknowledged cause of DEEs. The gain-of-function molecular phenotype can explain the hypersensitive reaction to vigabatrin seen in our patients and caution is required when prescribing vigabatrin to patients with $GABA_A$

receptor variants. We propose that different molecular phenotypes will require different drug treatments targeted at the functional effect of the epilepsy-causing variant, paving the way for a precision medicine approach to the treatment of some forms of DEE.

Acknowledgements

We thank the families and patients that contributed to this study.

Funding

N.L.A. was supported by the Lambert Initiative for Cannabinoid Therapeutics, a philanthropically funded research centre at the University of Sydney. N.L.A., P.K.A., V.W.Y.L. and M.C. were supported by the Australian National Health and Medical Research Council (APP1185122 and APP1124567). Both V.W.Y.L. and P.K.A. were supported by the Australian Research Council of Australia (LP160100560). M.T.B. was supported by the Australian National Health and Medical Research Council (APP1092046). R.S.M. was supported by the Lundbeck Foundation (R324-2019-1083). I.S.M., M.C. and M.T.B. receive grants and salary support from the Lambert Initiative for Cannabinoid Therapeutics. Exome sequencing and analysis support for one of the three patient was provided by Broad Institute of MIT and Harvard Center for Mendelian Genomics funded by the National Institutes of Health grant UM1HG008900. A.M. and M.K. are supported by the National Institute for Health Research Great Ormond Street Hospital Biomedical Research Centre (NIHR GOSH BRC). The views expressed are those of the author(s) and not necessarily those of the NHS, the NIHR or the Department of Health.

Competing interests

M.C. receives funding from the Lambert Initiative for Cannabinoid Therapeutics, a philanthropically funded research centre at the University of Sydney M.C., N.A., K.K., P.A. received funding from the National Health and Medical Research Council of Australia, Ideas grant 1185122. ISM receives grants and salary support from National Health and Medical Research Council of Australia and from Lambert Initiative for Cannabinoid Therapeutics and has patents to WO2018107216A1, WO2017004674A1 and WO2011038451A1 issued and licensed; and patents to AU2017904438, AU2017904072 and AU2018901971 pending. None of the patents relate to the work presented in this manuscript. I.S.M. and M.T.B. also act as consultants for Kinoxis Therapeutics. A.M. receives grants and salary support from the NIHR GOSH BRC and Rosetrees Trust and received an honorarium from Biocodex. All other authors have nothing to disclose.

References

Absalom NL, Ahring PK, Liao VW, Balle T, Jiang T, Anderson LL, et al. Functional genomics of epilepsy-associated mutations in the GABAA receptor subunits reveal that one mutation impairs function and two are catastrophic. J Biol Chem 2019; 294: 6157–71.

Anstee QM, Knapp S, Maguire EP, Hosie AM, Thomas P, Mortensen M, et al. Mutations in the Gabrb1 gene promote alcohol consumption through increased tonic inhibition. Nat Commun 2013; 4: 2816.

Butler KM, Moody OA, Schuler E, Coryell J, Alexander JJ, Jenkins A, et al. *De novo* variants in GABRA2 and GABRA5 alter receptor function and contribute to early-onset epilepsy. Brain 2018; 141: 2392–405.

Chiron C, Dulac O. The pharmacologic treatment of Dravet syndrome. Epilepsia 2011; 52: 72–5.

Delahanty RJ, Kang JQ, Brune CW, Kistner EO, Courchesne E, Cox NJ, et al. Maternal transmission of a rare GABRB3 signal peptide variant is associated with autism. Mol Psychiatry 2011; 16: 86–96.

French JA. Refractory epilepsy: one size does not fit all. Epilepsy Curr 2006; 6: 177–80.

Fritschy JM, Benke D, Mertens S, Oertel WH, Bachi T, Möhler H. Five subtypes of type A gamma-aminobutyric acid receptors identified in neurons by double and triple immunofluorescence staining with subunit-specific antibodies. Proc Natl Acad Sci U S A 1992; 89: 6726–30.

Gataullina S, Bienvenu T, Nabbout R, Huberfeld G, Dulac O. Gene mutations in paediatric epilepsies cause NMDA-pathy, and phasic and tonic GABA-pathy. Dev Med Child Neurol 2019; 61: 891–8.

Gielen MC, Lumb MJ, Smart TG. Benzodiazepines modulate GABAA receptors by regulating the preactivation step after GABA binding. J Neurosci 2012; 32: 5707–15.

Hernandez CC, Macdonald RL. A structural look at GABAA receptor mutations linked to epilepsy syndromes. Brain Res 2019; 1714: 234–47.

Hernandez CC, XiangWei W, Hu N, Shen D, Shen W, Lagrange AH, et al. Altered inhibitory synapses in *de novo* GABRA5 and GABRA1 mutations associated with early onset epileptic encephalopathies. Brain 2019; 142: 1938–54.

Hernandez CC, Zhang Y, Hu N, Shen D, Shen W, Liu X, et al. gabaa receptor coupling junction and pore GABRB3 mutations are linked to early-onset epileptic encephalopathy. Sci Rep 2017; 7: 15903.

Hernández Vega Y, Kaliakatsos M, U-King-Im JM, Lascelles K, Lim M. Reversible vigabatrin-induced life-threatening encephalopathy. JAMA Neurol 2014; 71: 108–9.

Janve VS, Hernandez CC, Verdier KM, Hu N, Macdonald RL. Epileptic encephalopathy *de novo* GABRB mutations impair γ-aminobutyric acid type A receptor function. Ann Neurol 2016; 79: 806–25.

Johannesen K, Marini C, Pfeffer S, Møller RS, Dorn T, Niturad CE, et al. Phenotypic spectrum of GABRA1: from generalized epilepsies to severe epileptic encephalopathies. Neurology 2016; 87: 1140–51.

Kash TL, Dizon MJ, Trudell JR, Harrison NL. Charged residues in the beta2 subunit involved in GABAA receptor activation. J Biol Chem 2004; 279: 4887–93.

Kothur K, Holman K, Farnsworth E, Ho G, Lorentzos M, Troedson C, et al. Diagnostic yield of targeted massively parallel sequencing in children with epileptic encephalopathy. Seizure 2018; 59: 132–40.

Kuenzle C, Steinlin M, Wohlrab G, Boltshauser E, Schmitt B. Adverse effects of vigabatrin in Angelman syndrome. Epilepsia 1998; 39: 1213–5.

Laverty D, Desai R, Uchański T, Masiulis S, Stec WJ, Malinauskas T, et al. Cryo-EM structure of the human $\alpha1\beta3\gamma2$ GABAA receptor in a lipid bilayer. Nature 2019; 565: 516–20.

Liao VWY, Chua HC, Kowal NM, Chebib M, Balle T, Ahring PK. Concatenated gamma-aminobutyric acid type A receptors revisited: finding order in chaos. J Gen Physiol 2019; 151: 798–819.

Lien E, Våtevik AK, Østern R, Haukanes BI, Houge G. A second patient with a *de novo* GABRB1 mutation and epileptic encephalopathy. Ann Neurol 2016; 80: 311–2.

Lux AL, Edwards SW, Hancock E, Johnson AL, Kennedy CR, Newton RW, et al. The United Kingdom Infantile Spasms Study (UKISS) comparing hormone treatment with vigabatrin on developmental and epilepsy outcomes to age 14 months: a multicentre randomised trial. Lancet Neurol 2005; 4: 712–7.

Maljevic S, Møller RS, Reid CA, Pérez-Palma E, Lal D, May P, et al. Spectrum of GABAA receptor variants in epilepsy. Curr Opin Neurol 2019; 32: 183–90.

Masiulis S, Desai R, Uchański T, Serna Martin I, Laverty D, Karia D, et al. GABAA receptor signalling mechanisms revealed by structural pharmacology. Nature 2019; 565: 454–9.

Mattison KA, Butler KM, Inglis GAS, Dayan O, Boussidan H, Bhambhani V, et al. SLC6A1 variants identified in epilepsy patients reduce γ-aminobutyric acid transport. Epilepsia 2018; 59: e135–41.

Møller RS, Larsen LH, Johannesen KM, Talvik I, Talvik T, Vaher U, et al. Gene panel testing in epileptic encephalopathies and familial epilepsies. Mol Syndromol 2016; 7: 210–19.

Møller RS, Wuttke TV, Helbig I, Marini C, Johannesen KM, Brilstra EH, et al. Mutations in GABRB3: from febrile seizures to epileptic encephalopathies. Neurology 2017; 88: 483–92.

Mortensen M, Patel B, Smart TG. GABA potency at GABA(A) receptors found in synaptic and extrasynaptic zones. Front Cell Neurosci 2011; 6: 1.

Nasrallah FA, Balcar VJ, Rae CD. Activity-dependent gamma-aminobutyric acid release controls brain cortical tissue slice metabolism. J Neurosci Res 2011; 89: 1935–45.

Niturad CE, Lev D, Kalscheuer VM, Charzewska A, Schubert J, Lerman-Sagie T, et al. Rare GABRA3 variants are associated with epileptic seizures, encephalopathy and dysmorphic features. Brain 2017; 140: 2879–94.

Nusser Z, Cull-Candy S, Farrant M. Differences in synaptic GABA(A) receptor number underlie variation in GABA mini amplitude. Neuron 1997; 19: 697–709.

Ortinski PI, Turner JR, Barberis A, Motamedi G, Yasuda RP, Wolfe BB, et al. Deletion of the GABA(A) receptor alpha1 subunit increases tonic GABA(A) receptor current: a role for GABA uptake transporters. J Neurosci 2006; 26: 9323–31.

Otis TS, Mody I. Modulation of decay kinetics and frequency of GABAA receptor-mediated spontaneous inhibitory postsynaptic currents in hippocampal neurons. Neuroscience 1992; 49: 13–32.

Papandreou A, McTague A, Trump N, Ambegaonkar G, Ngoh A, Meyer E, et al. GABRB3 mutations: a new and emerging cause of early infantile epileptic encephalopathy. Dev Med Child Neurol 2016; 58: 416–20.

Pavlov I, Walker MC. Tonic GABA(A) receptor-mediated signalling in temporal lobe epilepsy. Neuropharmacology 2013; 69: 55–61.

Persohn E, Malherbe P, Richards JG. Comparative molecular neuroanatomy of cloned GABAA receptor subunits in the rat CNS. J Comp Neurol 1992; 326: 193–216.

Phulera S, Zhu H, Yu J, Claxton DP, Yoder N, Yoshioka C, et al. Cryo-EM structure of the benzodiazepine-sensitive $\alpha1\beta1\gamma2S$ tri-heteromeric GABAA receptor in complex with GABA. elife 2018; 7: pii:e39383.

Pirker S, Schwarzer C, Wieselthaler A, Sieghart W, Sperk G. GABA(A) receptors: immunocytochemical distribution of 13 subunits in the adult rat brain. Neuroscience 2000; 101: 815–50.

Plested AJ, Groot-Kormelink PJ, Colquhoun D, Sivilotti LG. Single-channel study of the spasmodic mutation alpha1A52S in recombinant rat glycine receptors. J Physiol 2007; 581: 51–73.

Shen D, Hernandez CC, Shen W, Hu N, Poduri A, Shiedley B, et al. *De novo* GABRG2 mutations associated with epileptic encephalopathies. Brain 2017; 140: 49–67.

Sigel E, Ernst M. The benzodiazepine binding sites of GABAA receptors. Trends Pharmacol Sci 2018; 39: 659–71.

Steudle F, Rehman S, Bampali K, Simeone X, Rona Z, Hauser E, et al. A novel *de novo* variant of GABRA1 causes increased sensitivity for GABA in vitro. Sci Rep 2020; 10: 2379.

Tanaka M, DeLorey TM, Delgado-Escueta A, Olsen RW. GABRB3, epilepsy, and neurodevelopment. In: JL Noebels, M Avoli, MA Rogawski, RW Olsen, AV Delgado-Escueta, editors. Jasper's basic mechanisms of the epilepsies. 4th edn. Bethesda, MD: National center for biotechnology information (US); 2012.

Wirrell EC, Laux L, Donner E, Jette N, Knupp K, Meskis MA, et al. Optimizing the diagnosis and management of Dravet syndrome: recommendations from a North American Consensus Panel. Pediatr Neurol 2017; 68: 18–34.

Wisden W, Seeburg PH. GABAA receptor channels: from subunits to functional entities. Curr Opin Neurobiol 1992; 2: 263–9.

Wu Y, Wang W, Richerson GB. GABA transaminase inhibition induces spontaneous and enhances depolarization-evoked GABA efflux via reversal of the GABA transporter. J Neurosci 2001; 21: 2630–9.

Wu Y, Wang W, Richerson GB. Vigabatrin induces tonic inhibition via GABA transporter reversal without increasing vesicular GABA release. J Neurophysiol 2003; 89: 2021–34.